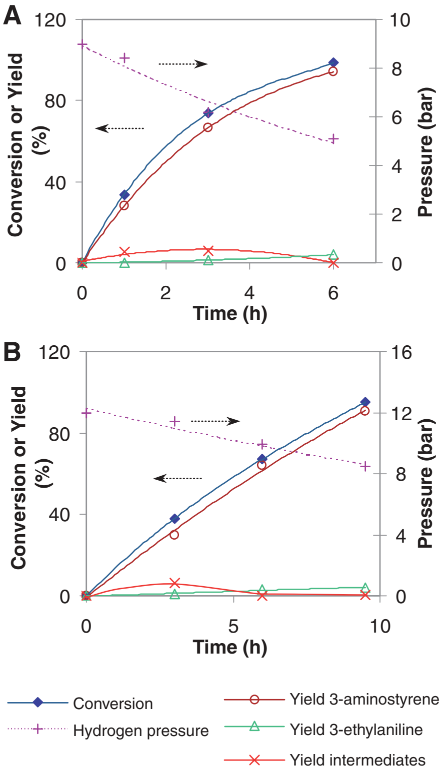

Fig. 1. Kinetic curves for 3-nitrostyrene hydrogenation with (**A**) Au/TiO_2 and (**B**) Au/Fe_2O_3 catalysts. Up to nearly 100% of conversion both catalytic systems provide selectivity >95%, avoiding the hydroxylamine accumulation problem (reaction conditions: for Au/TiO_2, 120°C, 9 bar, and 0.23 mol % of Au; for Au/Fe_2O_3, 130°C, 12 bar, and 0.39 mol % of Au). Arrows indicate that the hydrogen pressure curve is referred to the right *y* axis, and the remaining curves are referred to the left *y* axis.

Given the excellent chemoselectivity of gold for reducing nitro compounds, we explored this system as an alternative catalytic route for the production of cyclohexanone oxime, an important molecule in the production of ε-caprolactame. Cyclohexanone oxime is currently obtained via two different routes (Scheme 1A).

In these processes, hydroxylamine, which is a toxic and unstable product, has to be used or otherwise synthesized in situ by the Sumitomo and ENICHEM procedure. However, the high activity and selectivity of gold catalysts open the possibility for an alternative process that would involve the steps given in Scheme 1B. This process requires a catalyst that selectively hydrogenates 1-nitro-1-cyclohexene into cyclohexanone oxime. Whereas Pt and Pd produce low selectivity even at relatively low levels of conversions, selectivity >90% is achieved at practically 100% conversion with the gold catalysts (Table 1).

References and Notes

1. R. S. Dowing, P. J. Kunkeler, H. van Bekkum, *Catal. Today* **37**, 121 (1997).
2. M. Suchy, P. Winternitz, M. Zeller, World (WO) Patent 91/00278 (1991).
3. F. Kovar, F. E. Armond, U.S. Patent 3,975,444 (1976).
4. J. Butera, J. Bagli, WO Patent 91/09023 (1991).
5. A. Burawoy, J. P. Critchley, *Tetrahedron* **5**, 340 (1959).
6. R. Braden, H. Knupfer, S. Hartung, U.S. Patents 4,002,673 and 4,051,177 (1977).
7. M. A. Narendra, O. P. Shivanand, D. R. Madhukar, WO Patent 2005.070.869 (2005).
8. W. Gerhar *et al.*, U.S. Patent 6,395,934 (2002).
9. P. N. Rylander, *Catalytic Hydrogenation in Organic Synthesis* (Academic Press, New York, 1979), p. 122.
10. U. Siegrist, P. Baumeister, H.-U. Blaser, *Catalysis of Organic Reactions*, F. Herkes, Ed., vol. 75 of *Chemical Industries* (Dekker, New York, 1998).
11. H.-U. Blaser, U. Siegrist, H. Steiner, in *Aromatic Nitro Compounds: Fine Chemicals through Heterogeneous Catalysis*, R. A. Sheldon, H. van Bekkum, Eds. (Wiley-VCH, Weinheim, Germany, 2001), p. 389.
12. E. Janin, *J. Catal.* **215**, 243 (2003).
13. P. Concepcion, A. Corma, J. Silvestre-Albero, *J. Am. Chem. Soc.* **126**, 5523 (2004).
14. A. Sepulveda-Escribano, F. Coloma, F. Rodriguez-Reinoso, *J. Catal.* **178**, 649 (1998).
15. A. Abad, P. Concepción, A. Corma, *Angew. Chem. Int. Ed. Engl.* **44**, 4066 (2005).
16. A. Corma, M. E. Domine, *Chem. Commun.* **32**, 4042 (2005).
17. S. Naito, M. Tanimoto, *J. Chem. Soc. Chem. Commun.* **12**, 832 (1988).
18. S. A. Blankenship, A. Rokicki, J. A. Perkins, U.S. Patent 2003.232.719 (2003).
19. C. Milone *et al.*, *J. Catal.* **236**, 80 (2005).
20. C. González-Arellano, A. Corma, M. Iglesias, *Chem. Commun.* **15**, 3451 (2005).
21. P. Claus, *Appl. Catal. Gen.* **291**, 222 (2005).
22. J. E. Bailie, G. J. Hutchings, *Chem. Commun.* **21**, 2151 (1999).
23. M. Ch. Daniel, D. Astruc, *Chem. Rev.* **104**, 293 (2004).
24. X. Lu, X. Xu, N. Wang, *J. Phys. Chem. A* **103**, 10969 (1999).
25. Materials and methods are available as supporting material on *Science* Online.
26. Detailed product distributions with the different catalysts are given in tables S1 to S6.
27. We thank the World Gold Council for supplying the gold catalysts that were used as well as for the corresponding transmission electron microscopy images and F. Sánchez, M. Iglesias, and C. González-Arellano for useful comments. This work was supported by Ministerio de Educación y Ciencia (grant MAT2003-07945-C02-01).

Supporting Online Material
www.sciencemag.org/cgi/content/full/313/5785/332/DC1
Materials and Methods
SOM Text
Figs. S1 to S3
Tables S1 to S6
Schemes S1 and S2
References

5 April 2006; accepted 7 June 2006
10.1126/science.1128383

A Dielectric Polymer with High Electric Energy Density and Fast Discharge Speed

Baojin Chu,[1,2] Xin Zhou,[3] Kailiang Ren,[3] Bret Neese,[1,2] Minren Lin,[2] Qing Wang,[1,2] F. Bauer,[4] Q. M. Zhang[1,2,3]*

Dielectric polymers with high dipole density have the potential to achieve very high energy density, which is required in many modern electronics and electric systems. We demonstrate that a very high energy density with fast discharge speed and low loss can be obtained in defect-modified poly(vinylidene fluoride) polymers. This is achieved by combining nonpolar and polar molecular structural changes of the polymer with the proper dielectric constants, to avoid the electric displacement saturation at electric fields well below the breakdown field. The results indicate that a very high dielectric constant may not be desirable to reach a very high energy density.

Dielectric materials are used to control and store charges and electric energies and play a key role in modern electronics and electric power systems. As the requirements grow for compact, low-cost electronic and electrical power systems, as well as for very high energy and power capacitive storage systems, the development of high power and energy density dielectric materials becomes a major enabling technology (*1*–*3*). For example, high energy density dielectric capacitors would help to reduce the volume, weight, and cost of the electric power system in hybrid electric vehicles.

Among various dielectric materials, polymers are presently the material of choice for energy storage applications because of their relatively high energy density, high electric breakdown field (E_b), low dielectric loss, fast speed, low cost, and graceful failure (i.e., high reliability) (*4*–*6*). However, dielectric polymers that are currently used for high energy density capacitors show low (<3) dielectric constants (represented by K). Consequently, the high energy density in the dielectric polymers relies on the high E_b (>500 MV/m). In general, the

---

[1] Materials Science and Engineering Department, [2] Materials Research Institute, Pennsylvania State University, University Park, PA 16802, USA. [3] Electrical Engineering Department, [4] Institute Franco-Allemand de Recherches, 5 Rue du General Cassagnou, 68300 Saint-Louis, France.

*To whom correspondence should be addressed. E-mail: qxz1@psu.edu

energy density of a dielectric material (shaded area in Fig. 1A) is equal to the integral $U_e = \int EdD$, where E is the electric field and D is the electric displacement or charge density. Therefore, besides a high E_b, a high D value is another key factor in achieving a high energy density. Furthermore, with a proper K to avoid the electric displacement saturation (D_{sat}) at fields well below E_b (early polarization saturation), an even higher electric energy density can be achieved (Fig. 1B).

In high energy density dielectric polymers that are presently used, the level of D is low. For biaxially oriented polypropylene, which has the highest energy density (~4 J/cm^3) among the known polymers, D is below 0.012 C/m^2 under a field of 600 MV/m. Conversely, in polymers with high dipole density, D values higher than 0.1 C/m^2 can be achieved, providing the potential of reaching an order of magnitude increase in the energy density (*7*). One such polar-polymer system is poly(vinylidene fluoride) (PVDF) and its copolymer with trifluoroethylene (TrFE), which is the best known ferroelectric polymer and has been used widely in electromechanical sensors and actuators (*7*–*10*). We show that, by combining the reversible nonpolar and polar molecular structural changes to realize high D with proper (or matched) K values to avoid the early D-saturation, a very high energy density (>17 J/cm^3) with fast discharge speed (<1 μs) and low dielectric loss can be obtained in defect-modified PVDF polymers.

A typical *D-E* loop for a P(VDF-TrFE) copolymer is shown (Fig. 2A). Owing to the high dipole density, the polymer displays a D_{sat} of ~0.1 C/m^2. Alternatively, the large remnant polarization in the normal ferroelectric PVDF and its copolymer P(VDF-TrFE) renders a small energy density (shaded area in Fig. 2A). Therefore, besides possessing a high D value, a polymer should also have very small remnant polarization ($D \approx 0$ at zero E), allowing for a large change in D. From the molecular point of view, in the normal ferroelectric phase of PVDF and P(VDF-TrFE), the polymer chains are already in the all-trans conformation (fig. S1A), and an applied field along the original D direction can only induce small changes in D (curve from point A to point B in Fig. 2A), which then lead to low energy density (*8*, *9*).

Recently, we demonstrated that by using defect modifications, the P(VDF-TrFE) copolymer at compositions below VDF/TrFE 70/30 mole percent (mol %) can be converted to a ferroelectric relaxor in which the remnant polarization is near zero and a large change in D can be obtained (*11*, *12*). A *D-E* loop for a terpolymer of VDF-TrFE–chlorofluoroethylene (CFE) 58.3/34.2/7.5 mol % is presented in Fig. 2A (*13*, *14*); CFE generates random defects in P(VDF-TrFE). Apparently, a much higher electric energy density can be achieved (upper shaded area in Fig. 2A). Integrating the discharge *D-E* curve (fig. S2) yields the electric energy density of the terpolymer. The terpolymer exhibits an electric energy density higher than 9 J/cm^3 under 400 MV/m field (Fig. 2B), which is higher than known polymers and other dielectric capacitors (*3*, *4*, *6*).

The discharged energy density of the terpolymer (Fig. 2B) increases in an almost linear fashion with E. This relationship contrasts with that of the linear dielectric polymer, in which the electric energy density is proportional to the square of E: $U_e = \frac{1}{2}K\varepsilon_0E^2$, where ε_0 is the vacuum permittivity ($\varepsilon_0 = 8.85 \times 10^{-12}$ F/m). Indeed, this is the effect of the early D-saturation in the terpolymer; the material reaches D-saturation at a field much lower than E_b, which reduces the energy density that can be stored in a dielectric material. As a quantitative estimation, we modeled the D-saturation as a reduction of the effective dielectric constant K_{eff} with the field (i.e., $U_e = \frac{1}{2}K_{eff}\varepsilon_0E^2$). The K_{eff} value was ~50 at low fields and decreased with E (Fig. 2B). At 400 MV/m, the terpolymer had a K_{eff} value of ~13.

In this sense, a very high K at low E is not a desirable feature for a dielectric material to achieve a very high electric energy density. Instead, a K that can maximize the electric energy density (curve II in Fig. 1B) is needed, even though that dielectric constant is lower than that of curve I. A piecewise response in D is used to approximate the real *D-E* response (Fig. 1B). This simple analysis illustrates the importance of a matched K to maximize the electric energy density.

In the relaxor ferroelectric polymer, the change in molecular conformation between the nonpolar and polar forms at room temperature is associated with the polar-glass transition process, which is accompanied by a broad and high K peak (*11*, *12*, *15*). Because the energy difference of PVDF homopolymer between the trans-gauche-trans-gauche′ (TGTG′) and all-trans conformations is very small, this may be used to generate a large change in D without the penalty of a high K at low E values (*16*, *17*). The TGTG′ and all-trans conformations as well as the associated α and β phases are illustrated in fig. S1. Recent simulations have shown that for the single molecular chain, a TGTG′ conformation has a lower energy value compared with the all-trans conformation; however, in the crystal-

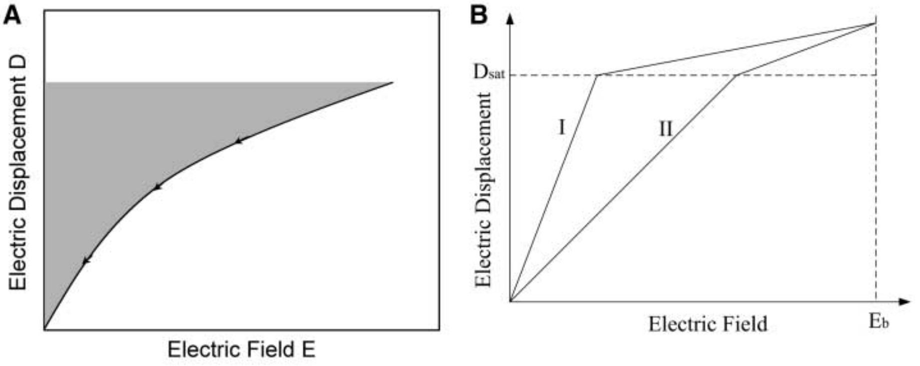

Fig. 1. (**A**) Schematic illustration of D and discharged energy density (shaded area) with E. Curve with arrows indicates energy release as the field is reduced. (**B**) Schematic illustration of the effect of K (the slope of *D-E* curve) on D_{sat} and energy density. The high K value of curve I leads to the early D-saturation and consequently to a lower energy density compared with that of curve II, despite its lower K value.

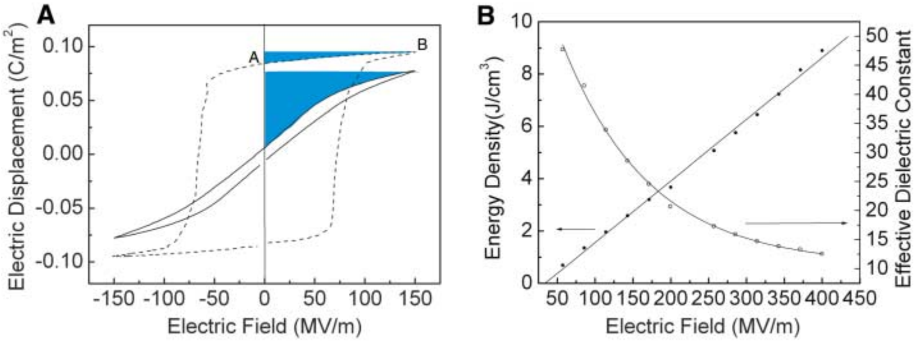

Fig. 2. (**A**) *D-E* loops for P(VDF-TrFE) 75/25 mol% (dotted lines) and P(VDF-TrFE–CFE) 58.3/34.2/7.5 mol% (solid lines) measured at 10 Hz. The shaded blue areas indicate the energy density. (**B**) The discharged energy density measured from the *D-E* loops and K_{eff} as a function of the field amplitude. The solid curves are drawn to guide eyes.

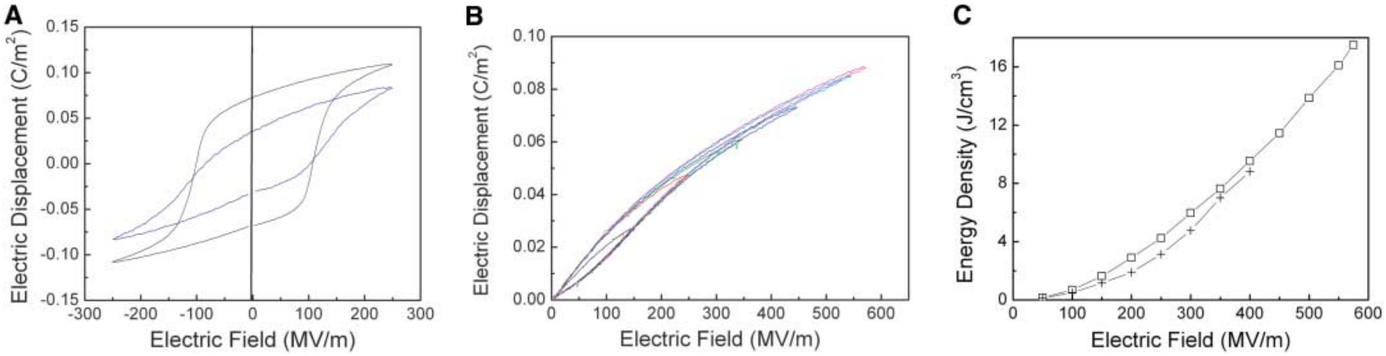

Fig. 3. (**A**) Comparison of the *D-E* loops of PVDF (black curves) and P(VDF-CTFE) 91/9 mol% (blue curves) measured at 10 Hz. P(VDF-CTFE) shows much lower remnant polarization even though the film was uniaxially stretched. (**B**) *D-E* loops measured under a unipolar *E* of 10 Hz for P(VDF-CTFE) 91/9 mol%. The different colored curves correspond to *D-E* loops measured with different field amplitudes. The conduction contribution was subtracted. (**C**) The discharged energy density measured from *D-E* loops under unipolar fields. Open squares, uniaxially stretched films; +, unstretched films. The uniaxially stretched P(VDF-CTFE) films exhibit much higher E_b values compared with unstretched films.

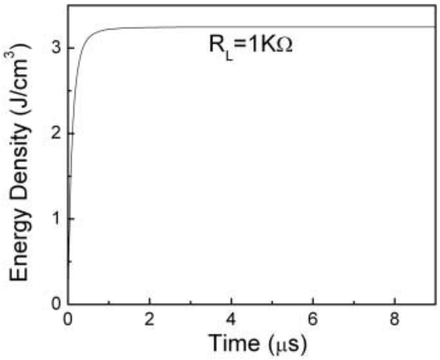

Fig. 4. Discharge energy density as a function of time measured from the direct discharge of the P(VDF-CTFE) polymer films to R_L of 1 kilohm. The *E* value is 253.5 MV/m.

line phase, the interchain coupling lowers the energy of the all-trans conformation with respect to the TGTG′ conformation (*17*). Therefore, defects that expand the interchain lattice spacing may lower the energy of the TGTG′ conformation and achieve a reversible change in conformations between the nonpolar and polar phases. This can also lead to a substantial change in *D* in the absence of a very high value of *K* at low *E* and the early *D*-saturation.

Based on these considerations, we examined random copolymers of VDF-chlorotrifluoroethylene (CTFE), in which the bulkier size of CTFE compared with VDF may expand the interchain space and distort the crystalline ordering (*14*). As previously observed for the PVDF homopolymer, the films prepared from the solution cast are in the α phase, whereas, after mechanical stretching, the films are converted to β phase, which is the thermodynamically lower energy phase for PVDF (*16*, *17*). In contrast, both of the films [P(VDF-CTFE) 91/9 mol%, unstretched and uniaxially stretched] exhibited an x-ray pattern of mostly the α phase (fig. S3), indicating that the small amount of bulky CTFE stabilizes the TGTG′ conformations and the α phase. In addition, the *D-E* hysteresis loop, measured from the uniaxially stretched P(VDF-CTFE) 91/9 mol% films, also exhibited much smaller remnant polarization as compared with that of PVDF (Fig. 3A).

The discharged energy density from the films of P(VDF-CTFE) 91/9 mol% was measured by the use of the Sawyer-Tower circuit under unipolar *E*s of 10 Hz (Fig. 3B) (*13*, *14*). The data indicate that P(VDF-CTFE) 91/9 mol% copolymer does not show *D*-saturation as seen in the terpolymers (fig. S2A). The discharged energy density as a function of *E* is presented in Fig. 3C, and the copolymer exhibited an energy density of more than 17 J/cm^3 under a field of 575 MV/m. Furthermore, the discharged energy density increased with the square of *E*, which suggests that, by improving the film quality so that E_b can be further raised to >575 MV/m, a much higher energy density can be achieved ($U_e \propto E^2$). For instance, E_b in the Langmuir-Blodgett films of P(VDF-TrFE) copolymer has been shown to be higher than 1000 MV/m (*18*).

For many applications to energy storage capacitors, a fast discharge time is required (*1*, *5*, *6*). We measured the discharge speed of these copolymer films by using a specially designed, high-speed capacitor discharge circuit in which the discharged energy was measured from a load resistor (R_L) in series with the polymer capacitor (fig. S4). For P(VDF-CTFE) capacitor films of 0.16 nF (measured at low field and 1 kHz) discharging to a 1 kilohm load, the energy discharging time is well below 1 μs (Fig. 4). As the R_L value changed from 1 to 100 kilohms, the discharge time increased by a factor of 100 (fig. S5). This finding indicates that the discharge time is controlled mainly by the capacitance of the film and external R_L and that the P(VDF-CTFE) copolymer capacitor can have very fast discharge time (<1 μs). Indeed, the fitting to the voltage change *V*(*t*) across the R_L yields the time constant that is nearly the same as that deduced from R_LC (fig. S6), where *C* is the capacitance. Furthermore, the discharged energy density does not change greatly when R_L is varied from 1 to 100 kilohms. These results show that the P(VDF-CTFE) copolymer capacitor possesses a low loss. Our demonstrated approach can also be applied to other polymers possessing high dipole density and high *D* to achieve ultra-high energy density with fast discharge time and low loss.

References and Notes

1. H. S. Nalwa, Ed., *Handbook of Low and High Dielectric Constant Materials and Their Applications*, *Vol. 2*, (Academic Press, New York, 1999).
2. Y. Cao, P. C. Irwin, K. Younsi, *IEEE Trans. Dielect. Elect. Insulation* **11**, 797 (2004).
3. W. Sarjeant, J. Zirnheld, F. MacDougall, *IEEE Trans. Plasma Sci.* **26**, 1368 (1998).
4. W. J. Sarjeant *et al*., in (*1*), chap. 9.
5. J. H. Tortai, N. Bonifaci, A. Denat, *J. Appl. Phys.* **97**, 053304 (2005).
6. M. Rabuffi, G. Picci, *IEEE Trans. Plasma Sci.* **30**, 1939 (2002).
7. H. S. Nalwa, Ed., *Ferroelectric Polymers* (Marcel Dekker, New York, 1995).
8. A. Lovinger, *Science* **220**, 1115 (1983).
9. Q. M. Zhang, V. Bharti, G. Kavarnos, in *The Encyclopedia of Smart Materials*, *Vol. 2*, M. Schwartz, Ed. (Wiley, New York, 2002).
10. T. T. Wang, J. M. Herbort, A. M. Glass, Eds., *The Applications of Ferroelectric Polymers* (Blackie, Glasgow, 1988).
11. Q. M. Zhang, V. Bharti, X. Zhao, *Science* **280**, 2101 (1998).
12. Q. M. Zhang, C. Huang, F. Xia, J. Su, in *Electroactive Polymer Actuators as Artificial Muscles*, Y. Bar-Cohen, Ed. (SPIE Press, Bellingham, WA, 2004), chap. 4.
13. J. K. Sinha, *J. Sci. Instrum.* **42**, 696 (1965).
14. Materials and methods are available as supporting material on *Science* Online.
15. V. Bobnar *et al.*, *Macromolecules* **36**, 4436 (2003).
16. R. G. Kepler, in (*7*), chap. 3.
17. H. Su, A. Strachan, W. Goddard III, *Phys. Rev.* **B70**, 064101 (2004).
18. A. V. Bune *et al.*, *Nature* **391**, 874 (1998).
19. This work was supported by the Office of Naval Research under grant numbers N00014-05-1-0455 and N00014-05-1-0541. We thank 3M for supplying P(VDF-CTFE) and PVDF powders used in this investigation.

Supporting Online Material

www.sciencemag.org/cgi/content/full/313/5785/334/DC1
Materials and Methods
Figs. S1 to S6
References

23 March 2006; accepted 13 June 2006
10.1126/science.1127798